CILAMCE 2017
Florianópolis - Santa Catarina - Brazil

ON A SIMPLE CODE FOR THE ACCURATE EVALUATION OF INTEGRALS IN THE 2D BOUNDARY ELEMENT METHOD USING ARBITRARILY HIGH ORDER, CURVED ELEMENTS

Ney Augusto Dumont

dumont@puc-rio.br

Department of Civil and Environmental Engineering
Pontifical Catholic University of Rio de Janeiro – PUC-Rio
22451-900 Rio de Janeiro, Brazil

Abstract. *This paper is the sequel of an article recently prepared, in which is shown that the traditional, collocation boundary element method (BEM) may undergo two decisive conceptual improvements for a generally curved boundary: (1) the interpolation function for normal fluxes or traction forces (for potential or elasticity problems) is redefined, and (2) only Gauss-Legendre quadrature turns out to be required. In the present paper, a simple, unified code is outlined for the arbitrarily highly accurate evaluation of the constituent matrices of 2D problems as well as of results at internal points independently from how convoluted a problem's topology may be (but given the representation limitations of a discretization mesh). A collateral, but not less relevant, outcome of the proposed developments is that regularization methods, special quadrature schemes and so many methods that intend to conceptually deviate from the originally stated BEM as an attempt to offer numerical improvements turn out to be mostly just misconceptions. A few numerical examples illustrate the high numerical accuracy one may arrive at in the frame of the present formulation.*

Keywords: *Boundary elements, numerical singularities, numerical quasi singularities.*

Proceedings of the XXXVIII Iberian Latin-American Congress on Computational Methods in Engineering
P.O. Faria, R.H. Lopez, L.F.F. Miguel, W.J.S. Gomes, M. Noronha (Editores), ABMEC, Florianópolis, SC, Brazil, November 5-8, 2017.

1 INTRODUCTION

This paper is basically the sequel of two research developments made by the author along the last few decades. The first research line deals with the adequate and accurate evaluation of the integrals occurring in a boundary element implementation [papers com Remo e Noronha]. The primary motivation was the accurate numerical evaluation of integrals in the frame of the hybrid, variationally-based boundary element method. However, this paper is devoted solely to the conventional, collocation boundary element method. The implementation proposed herein had its basic features already specifically addressed in two previous papers (Dumont, 1994; Dumont and Noronha, 1998) and starts by acknowledging that dealing with quasi singularities implies finding the complex roots of the basic equation $r^2(\xi)=0$. This is to the author's best knowledge the only feasible, mathematically consistent technique for the evaluation of general quasi singularities that occur in the boundary integral equation formulations. As shown in the present paper, the implementation results in a robust code and implies no additional computational effort. On the contrary, just a few numerical integration points turn out to be required for highly accurate results along curved boundaries. Moreover, the closer a source point is to an integration interval, the more accurate the numerical results become. It is shown that the evaluation of results at internal points – even if one is using the (singular) Kelvin's fundamental solution – requires dealing with high-order quasi singularities, which is a crucial issue in a numerically consistent boundary element implementation. In fact, if a numerical integration is carried out properly, as proposed, there is no need of regularizing a boundary element formulation – a procedure that in general leads to just a rough numerical approximation of the actual mathematical problem and sometimes creates more numerical troubles – as well as there is no need of trying to arrive at time-consuming analytical evaluations for some given particular configuration. The present developments cannot be outmatched in terms of simplicity and accuracy, as shown by means of several numerical examples.

The second research line deals with the collocation boundary element method, as derived on the basis of a weighted-residuals statement (Dumont, 2010). Only the static case is addressed, as it already involves all relevant conceptual issues. The outline presented by Dumont (2010) brings to discussion some relevant conceptual and implementation aspects of the method that should belong in any text book. It is shown that, if the boundary element method is consistently formulated, an inherent error term – related to arbitrary rigid-body displacements – is naturally taken into account in the implementation of the double-layer potential matrix **G**, so that boundary traction forces that are not in balance are automatically filtered out of the numerical solution independently of mesh discretization (Dumont, 1998). The constitutive matrices of the method – the single-layer and double-layer potential matrices **G** and **H** – turn out to display some spectral properties that are per se interesting but that also have applicability consequences. The matrix **G** is rectangular, if consistently obtained. For an adequately formulated problem, the solution of the resultant matrix equation is always possible (and unique). For the sake of brevity this spectrally consistent formulation will not be addressed in the present paper and interested readers are referred to (Dumont, 1998, 2010). The present paper also introduces a novel proposition for the interpolation of traction forces along curved boundaries, with results that were considered by Dumont (2010) as just a slight improvement, as compared to the classical procedure, but which turns out to be a decisive step towards attaining a numerically perfect code.

The present paper follows closely and also extends a presentation made by the author during the BEM/MRM 2017 as a tribute to the 40th anniversary of this pioneering sequence of conferences organized by Prof. Carlos Brebbia in the area of the boundary element methods (Dumont, 2017).

2 PROBLEM FORMULATION

The developments of this Section are classic in the literature except for some conceptual improvements done by the author. It seems appropriate to just follow and almost literally repeat the introduction of Dumont (2017).

As applied to an elastostatics problem, the single-layer and double-layer potential matrices $\mathbf{G}$ and $\mathbf{H}$ of the BEM are obtained as

$$\mathbf{Hd} = \mathbf{Gt} \tag{1}$$

(body forces not considered, for simplicity) for nodal displacements $\mathbf{d}$ and boundary nodal traction attributes $\mathbf{t}$. This equation turns out to be an application of Somigliana's identity that converts boundary data into domain displacements (Dumont, 2010). Whenever the boundary data are inaccurate, as the result of approximated values of $\mathbf{d} \equiv d_f$ and $\mathbf{t} \equiv t_\ell$ for a given problem as well as of the piecewise boundary interpolation, an error term $\boldsymbol{\varepsilon}$ should actually be added to this equation (Dumont, 1998). The matrices $\mathbf{G}$ and $\mathbf{H}$ are expressed in terms of the boundary integrals

$$\begin{aligned} G_{s\ell} &= \int_\Gamma u^*_{is}(\mathbf{x}-\mathbf{x}_s) t_{i\ell}(\mathbf{x}) \mathrm{d}\Gamma(\mathbf{x}) \\ H_{sf} &= \int_\Gamma \sigma^*_{jis}(\mathbf{x}-\mathbf{x}_s) n_j(\mathbf{x})\, u_{if}(\mathbf{x}) \mathrm{d}\Gamma(\mathbf{x}), \end{aligned} \tag{2}$$

where $u^*_{is}(\mathbf{x}-\mathbf{x}_s)$ and $\sigma^*_{jis}(\mathbf{x}-\mathbf{x}_s)$ are the displacement and stress (Kelvin's) fundamental solutions of the elastic problem – which have global support – and $\Gamma(\mathbf{x})$ is the integration boundary[1]. In the above equation and in the following, repeated indices mean summation. The vector $\mathbf{x} \equiv (x, y, z)$ stands for the Cartesian coordinates of a given point, in the case a field point, and $n_j(\mathbf{x}(\xi,\eta))$ are the Cartesian components of the unity outward vector $n(\mathbf{x}(\xi,\eta))$ to $\Gamma(\mathbf{x}(\xi,\eta))$, in terms of parametric variables (ξ,η), for a general 3D problem. The subscript s refers to a given source node (at which the unit point force of the singular fundamental solution is applied) and the subscripts f (which stands for field) and ℓ (also a field reference) indicate respectively to which node or surface point the displacement-interpolation function $u_{if}(\mathbf{x}(\xi,\eta))$ or the traction-interpolation function $t_{i\ell}(\mathbf{x}(\xi,\eta))$ – both with local support – are referred. $u_{if}(\mathbf{x}(\xi,\eta))$ comes from the piecewise interpolation of displacements $u_i(\mathbf{x}(\xi,\eta))$ along the boundary, $u_i(\mathbf{x}) = u_{if}(\mathbf{x}(\xi,\eta)) d_f$, where d_f are the nodal displacements. In a

[1] Since both interpolation functions $u_{if}(\mathbf{x}(\xi,\eta))$ and $t_{i\ell}(\mathbf{x}(\xi,\eta))$ formally introduced in eqn (2) have local support, there is no need of indicating that the boundary integrations are to be carried out segment by segment.

practical finite element or boundary element implementation, $u_{if}(\mathbf{x}(\xi,\eta))$ is actually represented by polynomial shape functions $N_f(\xi,\eta)$:

$$u_{if}(\mathbf{x}(\xi,\eta)) = \begin{cases} N_f(\xi,\eta) & \text{if } i \text{ and } f \text{ refer to the same Cartesian direction} \\ 0 & \text{otherwise.} \end{cases} \tag{3}$$

In the expression of $\mathbf{H}$, the Jacobian used in the definition of $n_j(\mathbf{x}(\xi,\eta))$ cancels out with the Jacobian of $\mathrm{d}\Gamma(\mathbf{x}) = |J(\xi,\eta)|\,\mathrm{d}\xi\mathrm{d}\eta$.

For the single-layer potential matrix $\mathbf{G}$, it is proposed that the usual (as found in the literature) interpolation polynomials $t_{i\ell}$ of traction forces $T_i(\mathbf{x}) = t_{i\ell}(\mathbf{x}(\xi,\eta))t_\ell$ in Eq. (2) be replaced with

$$t_{i\ell} = \frac{|J|_{(\text{at }\ell)}}{|J|} \begin{cases} N_\ell(\xi,\eta) & \text{if } i \text{ and } \ell \text{ refer to the same Cartesian direction} \\ 0 & \text{otherwise,} \end{cases} \tag{4}$$

where $|J|_{(\text{at }\ell)}$ is the value of the Jacobian at the point characterized by the subscript ℓ (Dumont, 2010). Nothing changes formally in the development of the BEM for curved boundary segments (and, of course, nothing changes numerically for the trivial cases of a constant Jacobian), except that the evaluation of $\mathbf{G}$ becomes much easier and actually more consistent as compared to proposed implementations given in the technical literature. In fact, $|J|$ cancels out in the product $t_{i\ell}\mathrm{d}\Gamma$ in Eq. (2) for $t_{i\ell}$ defined as suggested, and the integrand of $\mathbf{G}$ becomes just a polynomial that multiplies the assumed kernel u^*_{is}.

2.1 The misconception of *continuous* versus *discontinuous* elements

In a practical implementation, the same shape functions $N_i(\xi)$ (they might be different as a corollary of the theorem to be enounced next) are used in Eqs. (3) and (4), although the context differs conceptually, as $\mathbf{G}$, among other features, is in general a rectangular matrix (ℓ in general refers to a larger number of parameters than f). There is in fact a remarkable difference between the representation of boundary displacements according to $u_i(\mathbf{x}) = u_{if}(\mathbf{x}(\xi,\eta))d_f$ and the representation of boundary tractions according to $T_i(\mathbf{x}) = t_{i\ell}(\mathbf{x}(\xi,\eta))t_\ell$, namely that d_f are nodal parameters whereas t_ℓ are surface attributes: While $u_i(\mathbf{x}) = u_{if}(\mathbf{x}(\xi,\eta))d_f$ is single valued at a node f independently from the approaching direction (discontinuities due to a cracked domain not considered, for simplicity), in the case of ℓ referring to a corner point the traction forces $T_i(\mathbf{x}) = t_{i\ell}(\mathbf{x}(\xi,\eta))t_\ell$ [or normal gradients $q(\mathbf{x}) = t_\ell(\mathbf{x}(\xi,\eta))q_\ell$, for potential problems] depend on the direction from which the point is approached (that is, to which surface segment the point ℓ is meant to belong). As a result, attaching the precise meaning to the quantities at geometric locations characterized by the subscripts ℓ and f in the formulation of matrices $\mathbf{G}$ and $\mathbf{H}$ in Eq. (2), so that Eq. (1) becomes solvable, may not be trivial in a general mixed boundary (Cauchy) formulation. However, the dilemma continuous versus discontinuous elements should not be posed in a consistent formulation, as continuous elements in the definition of $\mathbf{G}$ simply stem from a misconception: while d_f and f are meant to refer to a nodal point, t_ℓ and ℓ should refer to just some surface point on a given boundary segment regardless the neighboring segments. (Observe for comparison that in a variational displacement formulation there is the concept of equivalent nodal forces p_f in such a way that $\mathbf{p}^{\mathrm{T}}\mathbf{d} \equiv p_f d_f$ means virtual work. This is by far not the case in the collocation BEM.)

The conceptual advantage of using the definition of Eq. (4) – and the eventual need of having the same functions $N_i(\xi)$ in both Eqs. (3) and (4) – becomes clear from the following theorem.

3 THEOREM ON THE ACCURATE REPRESENTATION OF CONSTANT STRESS STATES

Theorem. For 2D problems with the boundary represented by piecewise, generally curved segments, the boundary element Eqs. (1)-(4) are able to exactly simulate constant stress state fields in the frame of an isoparametric formulation. For 3D problems, constant stress states are exactly simulated only if the boundary geometry is piecewise represented by up to second degree polynomials (constant, linear and quadratic triangular as well as linear quadrilateral boundary elements).

The proof of this theorem is too lengthy to be presented here. Interested readers are referred to Dumont (2017) as well as to a comprehensive paper that shall be published shortly. The first part of this proof actually coincides with the proof required in the displacement finite element method, as firstly proposed by Bazeley et all (1965) – see also Zienkiewicz (1977).

4 ACCURATE NUMERICAL EVALUATION OF MATRIX $\mathbf{G}$ FOR POTENTIAL PROBLEMS

Although the present developments are seamlessly applicable to two-dimensional elasticity problems, owing to space restrictions only the simpler case of a potential problem (solution of the Laplace equation with material property $k=1$) is outlined.

The matrix $\mathbf{G}$ is to be evaluated as in Eq. (2) along a boundary segment Γ_{seg} for an interpolation function given according to Eq. (4) by $|J|_{(\text{at}\,n)} N_n^{o_e}(\xi) \big/ |J(\xi)|$, where $n=1\ldots o_e+1$ is the local numbering ℓ of the boundary segment and o_e is the degree of the interpolation polynomial $N_n^{o_e}(\xi)$.

4.1 Evaluation of $\mathbf{G}$ for the improper integral

One uses $u_m^*(\mathbf{x}-\mathbf{x}_m) = -\ln|\mathbf{x}(\xi)-\mathbf{x}(\xi_m)|/2\pi \equiv -\ln|r_m(\xi-\xi_m)|/2\pi \equiv -\ln r_m/2\pi$, where $0 \le \xi_m \le 1$ is the parametric coordinate of the source point s, which is locally numbered $m=1\ldots o_e+1$, for o_e+1 source points along Γ_{seg}. (Implementations using $0 \le \xi_m \le 1$ turn out to be simpler than for $-1 \le \xi_m \le 1$.) Then, a submatrix of $G_{s\ell}$ locally numbered as G_{mn} is evaluated as

$$2\pi G_{mn} = -\int_{\Gamma_{seg}} \ln r_m \frac{|J|_{(\mathrm{at}\, n)}}{|J(\xi)|} N_n^{o_e}(\xi)\,\mathrm{d}\Gamma(\xi) = -|J|_{(\mathrm{at}\, n)} \int_0^1 \ln r_m\, N_n^{o_e}\,\mathrm{d}\xi\,, \tag{5}$$

which is the same as (no summation over repeated indices)

$$\begin{aligned}
\frac{-2\pi}{|J|_{(\mathrm{at}\, n)}} G_{mn} &= \int_0^1 \ln\left|\frac{r_m}{\xi-\xi_m}\right| N_n^{o_e}\,\mathrm{d}\xi + \int_0^1 \ln|\xi-\xi_m|\, N_n^{o_e}\,\mathrm{d}\xi \\
&\simeq GL\int_0^1 \ln\left|\frac{r_m}{\xi-\xi_m}\right| N_n^{o_e}\,\mathrm{d}\xi + \int_0^1 \ln|\xi-\xi_m|\, N_n^{o_e}\,\mathrm{d}\xi \\
&= GL\int_0^1 \ln r_m\, N_n^{o_e}\,\mathrm{d}\xi + \left(\int_0^1 \ln|\xi-\xi_m|\, N_n^{o_e}\,\mathrm{d}\xi - GL\int_0^1 \ln|\xi-\xi_m|\, N_n^{o_e}\,\mathrm{d}\xi\right).
\end{aligned} \tag{6}$$

In this equation, the symbol GL is introduced to mean a Gauss-Legendre quadrature using a given number n_g of evaluation points, which is applicable to the indicated evaluation in the second row up to a desired accuracy, and then split in the third row. Observe that, in this third row, one obtains the intended evaluation of the integral of Eq. (5) as if carried out in the frame of a Gauss-Legendre quadrature plus the correction term given in brackets. This correction term is an array with o_e+1 constants that only depend on the shape function $N_n^{o_e}$ and can be previously evaluated for a given number n_g of Gauss-Legendre points and stored. The analytical part of this correction term can be already expressed as an array of $(o_e+1)\times(o_e+1)$ matrices, whose rows and columns correspond to the shape functions $N_n^{o_e}$ and singularity poles ξ_m, respectively, as illustrated for constant, linear, quadratic and cubic elements:

$$\int_0^1 \ln|\xi-\xi_m|\, N_n^{o_e}\,\mathrm{d}\xi := \left\{ 1 = \begin{bmatrix} \frac{-3}{4} & \frac{-1}{4} \\ \frac{-1}{4} & \frac{-3}{4} \end{bmatrix},\quad 2 = \begin{bmatrix} \frac{-17}{36} & \frac{-\ln 2}{6}-\frac{1}{18} & \frac{1}{36} \\ \frac{-5}{9} & \frac{-2\ln 2}{3}-\frac{8}{9} & \frac{-5}{9} \\ \frac{1}{36} & \frac{-\ln 2}{6}-\frac{1}{18} & \frac{-17}{36} \end{bmatrix}, \right.$$

$$\left. 3 = -\begin{bmatrix} \frac{11}{32} & \frac{\ln 3}{8}+\frac{1}{32} & \frac{\ln 3}{8}+\frac{1}{96}-\frac{\ln 2}{9} & \frac{1}{32} \\ \frac{19}{32} & \frac{3\ln 3}{8}+\frac{67}{96}-\frac{\ln 2}{9} & \frac{3\ln 3}{8}+\frac{25}{96}-\frac{4\ln 2}{9} & \frac{1}{32} \\ \frac{1}{32} & \frac{3\ln 3}{8}+\frac{25}{96}-\frac{4\ln 2}{9} & \frac{3\ln 3}{8}+\frac{67}{96}-\frac{\ln 2}{9} & \frac{19}{32} \\ \frac{1}{32} & \frac{\ln 3}{8}+\frac{1}{96}-\frac{\ln 2}{9} & \frac{\ln 3}{8}+\frac{1}{32} & \frac{11}{32} \end{bmatrix},\quad 0 = \left[-\ln 2 - 1\right] \right\} \tag{7}$$

4.2 Evaluation of $\mathbf{G}$ for complex and real quasi-singularities

When the source point $\mathbf{x}_s$ is not on the integration segment Γ_{seg} but sufficiently close to configure a quasi-singularity, one evaluates ξ_s such that $r^2(\xi-\xi_s)\equiv r^2=0$ and obtains

$$r^2=\left(x(\xi_s)-x_s\right)^2+\left(y(\xi_s)-y_s\right)^2=\rho(\xi)w(\xi_s)\equiv\rho(\xi)\left[(\xi_s-a)^2+b^2\right]=0 \tag{8}$$

where $w(\xi)\equiv w=(\xi-a)^2+b^2$ has roots $\xi_s=a\pm bi$, with $i=\sqrt{-1}$, and $\rho(\xi)$ is a polynomial whose degree depends on o_e and has only complex roots of large values. Then, $\xi_s=a\pm bi$ characterizes the complex quasi-singularity one must deal with. The evaluation of (a,b) is not trivial and must be carried out iteratively using a Newton-Raphson algorithm, for instance, as given by Dumont (1994) for quadratic elements, and generalized in the present developments for an element of arbitrary order o_e. The explicit evaluation of $\rho(\xi)$ in $r^2(\xi)=\rho(\xi)w(\xi)$ can be circumvented by simply expressing $\rho=r^2/w$.

Complex quasi-singularity. In such a case, one may write from Eq. (5)

$$\begin{aligned}\frac{-4\pi}{|J|_{(\text{at }n)}}G_{mn}&=\int_0^1\ln\left(\frac{r^2}{w}\right)N_n^{o_e}\,\mathrm{d}\xi+\int_0^1\ln(w)\,N_n^{o_e}\,\mathrm{d}\xi\\&\simeq GL\int_0^1\ln r^2N_n^{o_e}\,\mathrm{d}\xi+\left(\int_0^1\ln(w)N_n^{o_e}\,\mathrm{d}\xi-GL\int_0^1\ln(w)N_n^{o_e}\,\mathrm{d}\xi\right).\end{aligned} \tag{9}$$

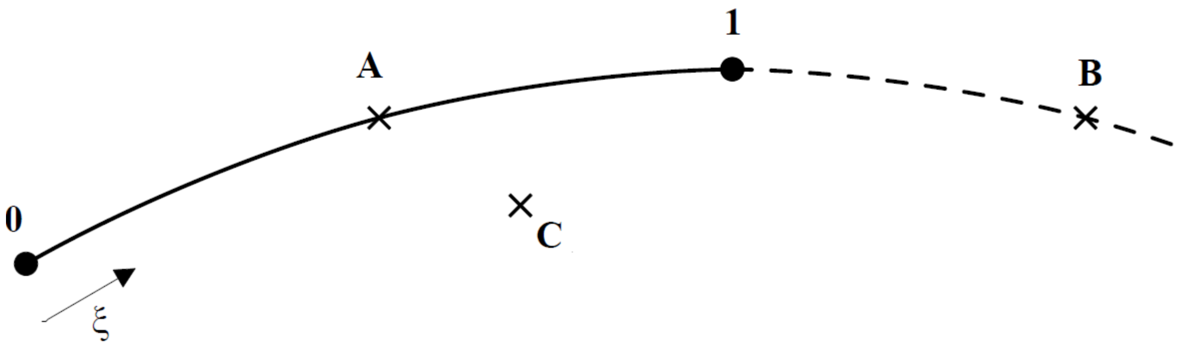

Figure 1. Illustration of a curved element with singularity points that can be real (point A), real quasi-singular (point B) and complex quasi-singular (point C) in terms of the parametric variable ξ

The definite integral $\int_0^1\ln(w)N_n^{o_e}\mathrm{d}\xi$, $n=1\ldots o_e+1$, for shape functions $N_n^{o_e}$ of order o_e, may be expressed as

$$\begin{aligned}\int_0^1\ln(w)N_n^{o_e}\mathrm{d}\xi&=\mathbf{L}_0^w\ln\left(a^2+b^2\right)+\mathbf{L}_1^w\ln\left((a-1)^2+b^2\right)\\&\quad+\mathbf{A}^w\left(\arctan\frac{a-1}{b}-\arctan\frac{a}{b}\right)+\mathbf{P}^w,\end{aligned} \tag{10}$$

where $\mathbf{L}_0^w$, $\mathbf{L}_1^w$, $\mathbf{A}^w$ and $\mathbf{P}^w$ are arrays with o_e+1 low order polynomial terms in a and b that fulfill the properties (since $N_i^{o_e}$ is a partition of unity):

$$\sum_{n=1}^{o_e+1} P^w[n] = -2, \quad \sum_{n=1}^{o_e+1} L_0^w[n] = a, \quad \sum_{n=1}^{o_e+1} L_1^w[n] = 1-a, \quad \sum_{n=1}^{o_e+1} A^w[n] = -2b\,. \tag{11}$$

Using the abbreviations $\Delta = b^2 - a^2$, $\Delta_1 = \Delta + 2b^2$, $\Delta_2 = \Delta + 4b^2$, the arrays above are given, for columns corresponding to constant, linear, quadratic and cubic elements, as

$$\mathbf{P}^w = \begin{bmatrix} -2 & a-\frac{3}{2} & \frac{4\Delta+7a}{3}-\frac{17}{18} & \frac{13-9\Delta_1}{4}a+\frac{39\Delta}{8}-\frac{11}{16} \\ \cdot & -a-\frac{1}{2} & -\frac{8\Delta+8a}{3}-\frac{10}{9} & \frac{27\Delta_1-15}{4}a-\frac{93\Delta}{8}-\frac{19}{16} \\ \cdot & \cdot & \frac{4\Delta+a}{3}+\frac{1}{18} & \frac{3-27_1}{4}a+\frac{69\Delta}{8}-\frac{1}{16} \\ \cdot & \cdot & \cdot & \frac{9\Delta_1-1}{4}a-\frac{15\Delta}{8}-\frac{1}{16} \end{bmatrix}. \tag{12}$$

$$\mathbf{L}_0^w = \begin{bmatrix} a & a+\frac{\Delta}{2} & \frac{3-2\Delta_1}{3}a+\frac{3\Delta}{2} & (1-3\Delta_1)a+\frac{9b^4}{2}+\frac{22-9\Delta_2}{8}\Delta \\ \cdot & -\frac{\Delta}{2} & \frac{4\Delta_1}{3}a-2\Delta & \frac{15\Delta_1}{2}a-\frac{27b^4}{2}-\frac{36-27\Delta_2}{8}\Delta \\ \cdot & \cdot & \frac{-2\Delta_1}{3}a+\frac{\Delta}{2} & -6\Delta_1 a+\frac{27b^4}{2}+\frac{18-27\Delta_2}{8}\Delta \\ \cdot & \cdot & \cdot & \frac{(3\Delta-2a)^2-(6ab-2b)^2}{8} \end{bmatrix}. \tag{13}$$

$$\mathbf{L}_1^w = \begin{bmatrix} 1-a & \frac{1-2a-\Delta}{2} & \frac{2\Delta_1-1}{3}a-\frac{3\Delta}{2}+\frac{1}{6} & \frac{(3\Delta+4a-1)^2-(6ab-4b)^2}{8} \\ \cdot & \frac{\Delta+1}{2} & -\frac{4\Delta_1}{3}a+2\Delta+\frac{2}{3} & -\frac{15\Delta_1}{2}a+\frac{27b^4}{2}+\frac{36-27\Delta_2}{8}\Delta+\frac{3}{8} \\ \cdot & \cdot & \frac{2\Delta_1}{3}a-\frac{\Delta}{2}+\frac{1}{6} & 6\Delta_1 a-\frac{27b^4}{2}-\frac{18-27\Delta_2}{8}\Delta+\frac{3}{8} \\ \cdot & \cdot & \cdot & -\frac{3\Delta_1}{2}a+\frac{9b^4}{2}+\frac{8-9\Delta_2}{8}\Delta+\frac{1}{8} \end{bmatrix}. \tag{14}$$

$$\mathbf{A}^w = \begin{bmatrix} -2b & 2b(a-1) & \frac{6\Delta-4b^2+9a-3}{3}2b & b(3a-2)(1-3\Delta-4a) \\ \cdot & -2ab & \frac{-3\Delta+2b^2-3a}{3}8b & 3b\left((9\Delta-6)a+15\Delta-10b^2\right) \\ \cdot & \cdot & \frac{6\Delta-4b^2+3a}{3}2b & 3b\left((3-9\Delta)a+12\Delta-8b^2\right) \\ \cdot & \cdot & \cdot & b(3a-1)(3\Delta+2a) \end{bmatrix}. \tag{15}$$

Real quasi-singularity. This occurs as a particular case of the previous section, when $b=0$, that is, $\xi_s = a$. Then, equation (9) becomes

$$\begin{aligned} \frac{-4\pi}{|J|_{(\text{at } n)}} G_{mn} &= \int_0^1 \ln\left(\frac{r^2}{|\xi-a|}\right) N_n^{o_e}\,\mathrm{d}\xi + \int_0^1 \ln|\xi-a|\, N_n^{o_e}\,\mathrm{d}\xi \\ &\simeq GL\int_0^1 \ln r^2 N_n^{o_e}\,\mathrm{d}\xi + \left(\int_0^1 \ln|\xi-a|\, N_n^{o_e}\,\mathrm{d}\xi - GL\int_0^1 \ln|\xi-a|\, N_n^{o_e}\,\mathrm{d}\xi\right) \end{aligned} \tag{16}$$

and one may express the definite integral $\int_0^1 \ln|\xi-a|\, N_n^{o_e}\mathrm{d}\xi,\ n=1\ldots o_e+1$, for shape functions $N_i^{o_e}$ of order o_e, as

$$\int_0^1 \ln|\xi-a|\, N_n^{o_e}\mathrm{d}\xi = \left(a\mathbf{L}_0^a \ln|a| + (1-a)\mathbf{L}_1^a \ln|1-a| + \mathbf{P}^a\right), \tag{17}$$

where $\mathbf{L}_0^a$, $\mathbf{L}_1^a$ and $\mathbf{P}^a$ are arrays with o_e+1 low order polynomial terms in a that fulfill the properties (since $N_i^{o_e}$ is a partition of unity):

$$\sum_{n=1}^{o_e+1} P^a[n] = -1, \quad \sum_{n=1}^{o_e+1} L_0^a[n] = \sum_{n=1}^{o_e+1} L_1^a[n] = 1. \tag{18}$$

As in the previous section, the arrays above are given, for columns corresponding to constant, linear, quadratic and cubic elements, as

$$\mathbf{P}^a = \begin{bmatrix} -1 & \frac{a}{2}-\frac{3}{4} & -\frac{2a^2}{3}+\frac{7a}{6}-\frac{17}{36} & \frac{18a^2-30a+11}{32}(2a-1) \\ \cdot & -\frac{a}{2}-\frac{1}{4} & \frac{4a^2}{3}-\frac{4a}{3}-\frac{5}{9} & -\frac{27a^3}{8}+\frac{93a^2}{16}-\frac{15a}{8}-\frac{19}{32} \\ \cdot & \cdot & -\frac{2a^2}{3}+\frac{a}{6}+\frac{1}{36} & \frac{27a^3}{8}-\frac{69a^2}{16}+\frac{3a}{8}-\frac{1}{32} \\ \cdot & \cdot & \cdot & \frac{18a^2-6a-1}{32}(1-2a) \end{bmatrix}. \tag{19}$$

$$\mathbf{L}_0^a=\begin{bmatrix} 1 & -\frac{a}{2}+1 & \frac{2a^2}{3}-\frac{3a}{2}+1 & -\frac{3a^2-4a+2}{8}(3a-4) \\ \cdot & \frac{a}{2} & -\frac{2a-3}{3}2a & \frac{9a^2-20a+12}{8}3a \\ \cdot & \cdot & \frac{4a-3}{6}a & -\frac{9a^2-16a+6}{8}3a \\ \cdot & \cdot & \cdot & \frac{(3a-2)^2}{8}a \end{bmatrix}. \tag{20}$$

$$\mathbf{L}_1^a=\begin{bmatrix} 1 & -\frac{a}{2}+\frac{1}{2} & \frac{4a-1}{6}(a-1) & -\frac{(3a-1)^2}{8}(a-1) \\ \cdot & \frac{a}{2}+\frac{1}{2} & -\frac{2a+1}{3}2(a-1) & \frac{9a^2-2a-1}{8}3(a-1) \\ \cdot & \cdot & \frac{2a^2}{3}+\frac{a}{6}+\frac{1}{6} & -\frac{9a^2+2a+1}{8}3(a-1) \\ \cdot & \cdot & \cdot & \frac{3a^2-2a+1}{8}(3a+1) \end{bmatrix}. \tag{21}$$

One also may check that the particular cases $\int_0^1 \ln\xi\, N_i^{o_e}\mathrm{d}\xi$ and $\int_0^1 \ln(1-\xi) N_i^{o_e}\mathrm{d}\xi$ are implicit in the developments above as only $\mathbf{P}^a$ is not void and is a function of either $a=0$ or $a=1$. As a last remark, the developments in Eq. (17) are actually a particular case of the developments in Eq. (10) for $b=0$:

$$\mathbf{P}^w=2\mathbf{P}^a,\quad \mathbf{L}_0^w=a\mathbf{L}_0^a,\quad \mathbf{L}_1^w=(1-a)\mathbf{L}_1^a,\quad \mathbf{A}^w=0 \qquad \text{for } b=0. \tag{22}$$

5 ACCURATE NUMERICAL EVALUATION OF MATRIX H FOR POTENTIAL PROBLEMS

5.1 Evaluation of H for a $1/r$ singularity

The $1/r$ singularity related to the double-layer matrix $\mathbf{H}$ is already adequately dealt with in the technical literature. It is summarized in the following equation. For r_m^2 defined as in Eq. (8), where $0\le\xi_m\le 1$ is the parametric coordinate of the source point s, locally numbered for a given boundary segment Γ_{seg} as $m=1\ldots o_e+1$, one expresses the normal gradient to the boundary as $q_m^*(\mathbf{x}-\mathbf{x}_m)=-\left(\left(x(\xi)-x(\xi_m)\right)y'(\xi)-\left(y(\xi)-y(\xi_m)\right)x'(\xi)\right)/2\pi r_m^2$. Then, the contribution to matrix H_{sf} locally numbered for the segment Γ_{seg} as H_{mn} is evaluated as

$$H_{mn}=\int_{\Gamma_{seg}} q^*_{jm} n_j N_n^{o_e} \mathrm{d}\Gamma+\delta_{mn}=\frac{-1}{2\pi}\int_{\Gamma_{seg}}\begin{vmatrix} x_m & x' \\ y_m & y' \end{vmatrix} N_n^{o_e}\frac{d\xi}{r_m^2}\mathrm{d}\Gamma+\delta_{mn}$$
$$\simeq\frac{-1}{2\pi}GL\int_{\Gamma_{ext}}\begin{vmatrix} x_m & x' \\ y_m & y' \end{vmatrix} N_n^{o_e}\frac{d\xi}{r_m^2}+\left(1-\frac{\Delta\theta_m}{2\pi}\right)\delta_{mn} , \quad (23)$$

(no summation over repeated indices m) where $\Delta\theta_m$ is the angular jump from the left to right tangent at node m ($\Delta\theta_m=\pi$ for a smooth boundary)[2]. Since the indicated determinant is equivalent to $|r_m\times n||J|_{(\text{at m})}$, it follows that $\lim\limits_{\xi\to\xi_m}|r_m\times n|/r_m^2$ is actually indeterminate (not infinite), so that the indicated integral can be directly evaluated in terms of finite part, which is best carried out using simply a Gauss-Legendre quadrature. Moreover, this finite part integral is void when the segment Γ_{seg} is straight.

5.2 Evaluation of $\mathbf{H}$ for complex and real quasi-singularities

Referring to the expression of $r^2(\xi)=\rho(\xi)w(\xi)$ in Section 4.2 and the above definitions for the matrix $\mathbf{H}$, one may write for the contribution H_{mn} of matrix H_{sf} along Γ_{seg}:

$$H_{mn}=\frac{-1}{2\pi}\int_{\Gamma_{seg}}\frac{1}{w}\left[\left(xy'-yx'\right)N_n^{o_e}\frac{w}{r^2}\right]\mathrm{d}\xi$$
$$=\frac{-1}{2\pi}\int_0^1\frac{1}{w}\left[\left(xy'-yx'\right)N_n^{o_e}\frac{w}{r^2}\right]\mathrm{d}\xi\equiv\int_0^1\frac{g}{w}\mathrm{d}\xi\equiv\int_0^1\frac{1}{w}\left(\frac{fw}{r^2}\right)\mathrm{d}\xi. \quad (24)$$

According to Eq. (25) in (Dumont, 1994), writing $\xi_m=a\pm bi$ as the complex roots of $w\equiv w(\xi)=(\xi-a)^2+b^2=0$ one obtains

$$\int_0^1\frac{g}{w}\mathrm{d}\xi=\int_0^1\frac{g-r_1}{w}\mathrm{d}\xi+\int_0^1\frac{r_1}{w}\mathrm{d}\xi$$
$$\simeq GL\int_0^1\frac{g}{w}\mathrm{d}\xi+\left[\int_0^1\frac{r_1}{w}\mathrm{d}\xi-GL\int_0^1\frac{r_1}{w}\mathrm{d}\xi\right], \quad (25)$$

or

$$\int_0^1\frac{g}{w}\mathrm{d}\xi\simeq GL\int_0^1\frac{g}{w}\mathrm{d}\xi+C_1R_2+C_2R_1, \quad (26)$$

where the coefficients of $r_1=R_1+R_2\xi$ are obtained such that $g(\xi_0)-r_1(\xi_0)=0$:

---

[2] It is worth mentioning that, since this angular jump must be evaluated in terms of the $\arctan$ function and the results depend on the angular quadrant, the simplest and computationally most robust way of carrying out the evaluation is by substituting $\mathrm{frac}\left(2-\Delta\theta_m/2\pi\right)$ for the term in parentheses in the above equation (the function frac gives the fractional part of a number).

$$g(\xi_0) = R_1 + R_2(a+bi) \\ \Rightarrow \; R_2 = \Im\big(g(\xi_0)\big)/b, \quad R_1 = \Re\big(g(\xi_0)\big) - R_2 a \tag{27}$$

$$C_1 = \int_0^1 \frac{\xi \mathrm{d}\xi}{w} - \sum_{i=1}^{n} \frac{\xi_i h_i}{w_i}, \quad C_2 = \int_0^1 \frac{\mathrm{d}\xi}{w} - \sum_{i=1}^{n} \frac{h_i}{w_i}. \tag{28}$$

The integrals in the above equations are defined analytically as simply

$$\int_0^1 \frac{\xi \mathrm{d}\xi}{(\xi-a)^2+b^2} = \frac{1}{2}\ln\frac{(1-a)^2+b^2}{a^2+b^2} + \frac{a}{b}\left(\arctan\frac{1-a}{b} + \arctan\frac{a}{b}\right), \quad \text{for } b \neq 0 \tag{29}$$

$$\int_0^1 \frac{\mathrm{d}\xi}{(\xi-a)^2+b^2} = \frac{1}{b}\left(\arctan\frac{1-a}{b} + \arctan\frac{a}{b}\right), \quad \text{for } b \neq 0. \tag{30}$$

For a real quasi-singularity $\xi_m = a$, with $b = 0$, the integral to be obtained is

$$\int_0^1 \frac{g}{\xi-a}\mathrm{d}\xi \simeq GL\int_0^1 \frac{g}{\xi-a}\mathrm{d}\xi + R_0 C_0, \quad \text{for either } a<0 \text{ or } a>1, \tag{31}$$

where $R_0 = g(\xi_0)$ and

$$C_0 = \int_0^1 \frac{\mathrm{d}\xi}{\xi-a} - \sum_{i=1}^{n} \frac{h_i}{\xi_i - a} = a\ln\left|\frac{a-1}{a}\right| + 1 - \sum_{i=1}^{n} \frac{h_i}{\xi_i - a}. \tag{32}$$

6 ACCURATE EVALUATION OF RESULTS AT INTERNAL POINTS FOR POTENTIAL PROBLEMS

Since Eq. (1) is just an application of Somigliana's identity, if one assumes that the boundary data may be interpolated according to the shape functions $t_{i\ell}$ and u_{if} introduced in Eq. (2), for known nodal parameters t_ℓ and d_f, potential and displacement results at internal points are evaluated using the same procedures applied to matrices $\mathbf{G}$ and $\mathbf{H}$ for the particular case of complex quasi-singularity, as outlined for potential problems in Sections 4.2 and 5.2. The corresponding expression for a given internal point s is

$$u_s = -\frac{|J|_{at\,\ell}}{4\pi}\int_\Gamma \ln r_s^2 \, N_\ell^{o_e} \, \mathrm{d}\xi \, t_\ell + \frac{1}{2\pi}\int_\Gamma \frac{1}{r_s^2}\left(x_s y' - y_s x'\right) N_n^{o_e} \, \mathrm{d}\xi \, d_n, \tag{33}$$

as required for the subsequent developments (here and in the following no summation is assumed over repeated s, although the indicial notation should still hold, in general).

For internal gradients, a procedure to deal with $\int_0^1 g/w^2 \mathrm{d}\xi$ must be developed, whereas stress results also demand the development of an algorithm to deal with the more elaborate case $\int_0^1 g/w^3 \mathrm{d}\xi$. Such general developments were outlined by Dumont (1994) and have been especially coded in the frame of the present research work. They have resulted into black boxes that are straight forward to implement. Owing to space restrictions, only the basic developments are shown in the following sections.

6.1 Gradient evaluation at internal points: a case of $1/w^2$ complex quasi-singularity

The formulation for this case has been already presented by Dumont (1994) for a general function $g(\xi)$ and will be further developed in the following, although the complete outline demands more space than available in the present manuscript. One may write:

$$\begin{aligned}&\int_0^1 \frac{g}{w^2}\,\mathrm{d}\xi = \int_0^1 \frac{1}{w}\frac{g-r_1}{w}\,\mathrm{d}\xi + \int_0^1 \frac{r_1}{w^2}\,\mathrm{d}\xi \\ &= \int_0^1 \frac{1}{w}\left(\frac{g-r_1}{w} - r_2\right)\mathrm{d}\xi + \int_0^1 \left(\frac{r_1}{w^2} + \frac{r_2}{w}\right)\mathrm{d}\xi \\ &\simeq GL\int_0^1 \frac{g}{w^2}\,\mathrm{d}\xi + \left[\int_0^1 \left(\frac{r_1}{w^2} + \frac{r_2}{w}\right)\mathrm{d}\xi - GL\int_0^1 \left(\frac{r_1}{w^2} + \frac{r_2}{w}\right)\mathrm{d}\xi\right]\end{aligned} \quad . \tag{34}$$

The coefficients of $r_1 = R_1 + R_2\xi$ are given as in Eq. (27), and $r_2 = R_3 + R_4\xi$ is obtained such that $\left(g(\xi_0) - r_1(\xi_0)\right)/w(\xi_0) - r_2(\xi_0) = 0$:

$$\begin{aligned}&\lim_{\xi\to\xi_0} \frac{g-r_1}{w} = R_3 + R_4(a+bi) \quad \Rightarrow \quad \frac{g'(\xi_0) - R_2}{2bi} = R_3 + R_4(a+bi) \\ &\Rightarrow \quad R_4 = \frac{R_2 - \Re\left(g'(\xi_0)\right)}{2b^2} \quad \text{and} \quad R_3 = \frac{\Im\left(g'(\xi_0)\right)}{2b} - R_4 a\end{aligned} \quad . \tag{35}$$

As a result, Eq. (34) can be expressed for a computational implementation as:

$$\int_0^1 \frac{g}{w^2}\,\mathrm{d}\xi \simeq GL\int_0^1 \frac{g}{w^2}\,\mathrm{d}\xi + \sum_{j=1}^{4} C_j R_{5-j} \;. \tag{36}$$

where C_1 and C_2 are already given in eq. (28) and

$$C_3 = \int_0^1 \frac{\xi\mathrm{d}\xi}{w^2} - \sum_{i=1}^{n_g} \frac{\xi_i h_i}{w_i^2}, \quad C_4 = \int_0^1 \frac{\mathrm{d}\xi}{w^2} - \sum_{i=1}^{n_g} \frac{h_i}{w_i^2} \quad . \tag{37}$$

The integrals above are defined analytically as

$$\begin{aligned}\int_0^1 \frac{\xi\mathrm{d}\xi}{\left((\xi-a)^2 + b^2\right)^2} &= \frac{a-1}{2b^2\left((1-a)^2 + b^2\right)} \\ &+ \frac{a}{2b^3}\left(\arctan\frac{1-a}{b} + \arctan\frac{a}{b}\right), \quad \text{for } b \neq 0\end{aligned} \quad . \tag{38}$$

Proceedings of the XXXVIII Iberian Latin-American Congress on Computational Methods in Engineering
P.O. Faria, R.H. Lopez, L.F.F. Miguel, W.J.S. Gomes, M. Noronha (Editores), ABMEC, Florianópolis, SC, Brazil, November 5-8, 2017.

$$\int_0^1 \frac{\mathrm{d}\xi}{\left((\xi-a)^2+b^2\right)^2} = \frac{b^2-a^2+a}{2b^2(a^2+b^2)\left((1-a)^2+b^2\right)} + \frac{1}{2b^3}\left(\arctan\frac{1-a}{b}+\arctan\frac{a}{b}\right), \quad \text{for } b\neq 0 \,. \tag{39}$$

6.2 Developments for the $1/w^3$ complex quasi-singularity in elasticity

The basic formulation for this case has also been already presented by Dumont (1994) for a general function $g(\xi)$ and will be further developed in the following:

$$\begin{aligned}\int_0^1 \frac{g}{w^3}\,\mathrm{d}\xi &= \int_0^1 \frac{1}{w^2}\frac{g-r_1}{w}\,\mathrm{d}\xi + \int_0^1 \frac{r_1}{w^3}\,\mathrm{d}\xi = \int_0^1 \frac{1}{w^2}\left(\frac{g-r_1}{w}-r_2\right)\mathrm{d}\xi + \int_0^1\left(\frac{r_1}{w^3}+\frac{r_2}{w^2}\right)\mathrm{d}\xi \\ &= \int_0^1 \frac{1}{w}\left(\frac{g-r_1-wr_2}{w^2}-r_3\right)\mathrm{d}\xi + \int_0^1\left(\frac{r_1}{w^3}+\frac{r_2}{w^2}+\frac{r_3}{w}\right)\mathrm{d}\xi \\ &\simeq GL\int_0^1 \frac{g}{w^3}\,\mathrm{d}\xi + \left[\int_0^1\left(\frac{r_1}{w^3}+\frac{r_2}{w^2}+\frac{r_3}{w}\right)\mathrm{d}\xi - GL\int_0^1\left(\frac{r_1}{w^3}+\frac{r_2}{w^2}+\frac{r_3}{w}\right)\mathrm{d}\xi\right] .\end{aligned} \tag{40}$$

The coefficients of $r_1 = R_1 + R_2\xi$ and $r_2 = R_3 + R_4\xi$ are given in Eqs. (27) and (35), and $\left(g(\xi_0)-r_1(\xi_0)-w(\xi_0)r_2(\xi_0)\right)/w^2(\xi_0)-r_3(\xi_0)=0$ is used to obtain $r_3 = R_5 + R_6\xi$:

$$\begin{aligned}&\lim_{\xi\to\xi_0}\frac{g-r_1-wr_2}{w^2} = R_5 + R_6(a+bi) \\ &\Rightarrow\quad \frac{2R_4(a+3bi)+2R_3-g''(\xi_0)}{8b^2} = R_5+R_6(a+bi) \\ &\Rightarrow\quad R_6 = \frac{6R_4 b - \Im\left(g''(\xi_0)\right)}{8b^3} \quad \text{and} \quad R_5 = \frac{2R_4 a + 2R_3 - \Re\left(g''(\xi_0)\right)}{8b^2} - R_6 a \,.\end{aligned} \tag{41}$$

As a result, Eq. (40) can be expressed for a computational implementation as:

$$\int_0^1 \frac{g}{w^3}\,\mathrm{d}\xi \simeq GL\int_0^1 \frac{g}{w^3}\,\mathrm{d}\xi + \sum_{j=1}^{6} C_j R_{7-j} \,. \tag{42}$$

where C_1, C_2, C_3, C_4 are already given in Eqs. (28) and (37), and

$$C_5 = \int_0^1 \frac{\xi\mathrm{d}\xi}{w^3} - \sum_{i=1}^{n_g}\frac{\xi_i h_i}{w_i^3}, \quad C_6 = \int_0^1\frac{\mathrm{d}\xi}{w^3} - \sum_{i=1}^{n_g}\frac{h_i}{w_i^3} \,. \tag{43}$$

The integrals above are defined analytically, using $c = 1-a$, as

$$\int_0^1 \frac{\xi \mathrm{d}\xi}{\left((\xi-a)^2+b^2\right)^3} = \frac{3c^5-6c^4+(6b^2+3)c^3-9b^2c^2+(3b^2+5)b^2c+b^4}{8b^4(a^2+b^2)\left(c^2+b^2\right)^2} + \frac{3a}{8b^5}\left(\arctan\frac{c}{b}+\arctan\frac{a}{b}\right), \quad \text{for } b\neq 0 . \tag{44}$$

$$\int_0^1 \frac{\mathrm{d}\xi}{\left((\xi-a)^2+b^2\right)^3} = \frac{5b^6+(ac+3)b^4-ac(9ac-5)b^2+3a^3c^3}{8b^4(a^2+b^2)^2(c^2+b^2)^2} + \frac{3}{8b^5}\left(\arctan\frac{c}{b}+\arctan\frac{a}{b}\right), \quad \text{for } b\neq 0 . \tag{45}$$

The complete formulation requires the evaluation of $g(\xi_0)$, $g'(\xi_0)$ and $g''(\xi_0)$, as given in Eqs. (27), (35) and (41), for the different application cases, which can only be done in terms of limit for $\xi \to \xi_0$ by successively applying L´Hospital's rule. This has already been developed for all cases that appear in 2D implementation of potential and elasticity problems and is being prepared for publication.

7 TWO SIMPLE NUMERICAL ASSESSMENTS

Two simple numerical illustrations are given next in order to show how accurate the results may become when the numerical integral evaluations are carried out as proposed in this paper.

7.1 Multiply-connected domain discretized with 15 quadratic elements

Figure 2 shows a 2D domain discretized externally with 11 quadratic elements and four more elements to configure a hole. Nodes 27 and 28 of the hole are almost coincident with the external boundary. Moreover, nodes 12 and 29 are very close. Observe that, owing to the curvature of the element defined by nodes 27, 28 and 29, there is only a very thin layer of material between the internal and external boundaries. Eleven analytical fields,

$$\left\langle 1 \quad x \quad y \quad xy \quad x^2-y^2 \quad x^3-3xy^2 \quad -3x^2y+y^3 \quad x^4+y^4-6x^2y^2 \quad x^3y-xy^3 \quad \ln\Delta r_1 \quad \ln\Delta r_2 \right\rangle, \tag{46}$$

are applied and in each case the corresponding nodal potential and gradient values $\mathbf{d}$ and $\mathbf{t}$, for the domain cut out as in Fig. 2, are evaluated in order to test the accuracy of Eq. (1). Observe that the first analytical solution corresponds to a constant potential, for which ideally $\|\mathbf{Hd}\|=0$, since we are dealing with a finite domain. The corresponding error norm for all following applications is given as ε_0:

$$\varepsilon_0 = \frac{\|\mathbf{Hd}\|}{\|\|\mathbf{H}\|\mathbf{d}\|\|}; \quad \varepsilon_1 = \frac{\|\mathbf{Hd}-\mathbf{Gt}\|}{\|\mathbf{Hd}\|}. \tag{47}$$

The error norm ε_1 is related to the remaining potential fields, which are pairs of linear, quadratic, cubic and quartic polynomial analytical solutions of the Laplace equation, besides

Proceedings of the XXXVIII Iberian Latin-American Congress on Computational Methods in Engineering
P.O. Faria, R.H. Lopez, L.F.F. Miguel, W.J.S. Gomes, M. Noronha (Editores), ABMEC, Florianópolis, SC, Brazil, November 5-8, 2017.

two logarithmic solutions referred to sources applied at the points indicated by crosses in Fig. 2, with coordinates $(5,2)$ and $(25,20)$.

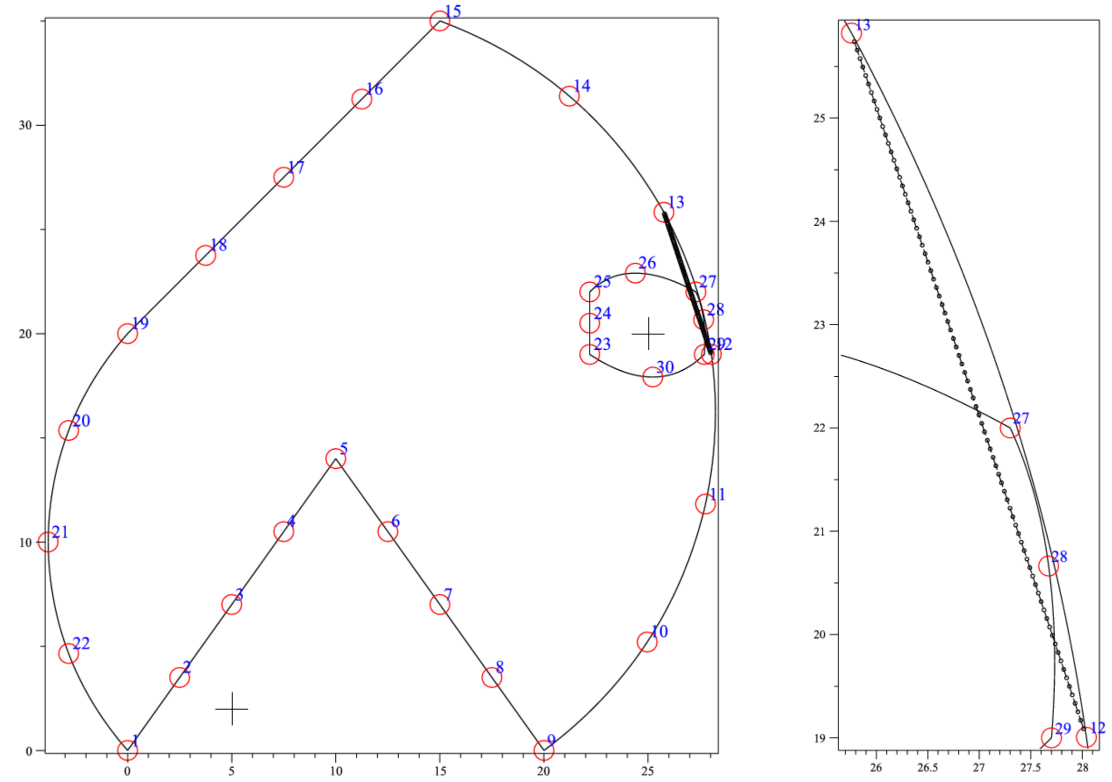

Figure 2. Multiply-connected domain discretized with a coarse mesh of 15 quadratic elements and dash line along which internal results are evaluated (enlarged part displayed on the right)

The matrices $\mathbf{G}$ and $\mathbf{H}$ were obtained using four Gaussian points per quadratic element for all calculations. The orthogonality of $\mathbf{H}$ with respect to a constant potential field was checked with global Euclidean error ε_0, as in Eq. (47), of 10^{-8}, which is the first value shown in the following equation:

$$\langle 0.1e{-6} \quad 0.2e{-5} \quad 0.2e{-5} \quad 0.4e{-2} \quad 0.2e{-2} \quad 0.1e{-1} \quad 0.1e{-1} \quad 0.3e{-1} \quad 0.2e{-1} \quad 0.5 \quad 0.3\rangle \tag{48}$$

In a second test with eight Gaussian points, the corresponding Euclidean error ε_0 was 10^{-13}, as shown in the following:

$$\langle 0.1e{-11} \quad 0.8e{-11} \quad 0.9e{-11} \quad 0.4e{-2} \quad 0.2e{-2} \quad 0.1e{-1} \quad 0.1e{-1} \quad 0.3e{-1} \quad 0.2e{-1} \quad 0.5 \quad 0.3\rangle \tag{49}$$

The remaining values in Eqs. (48) and (49) are Euclidean norms ε_1 defined in Eq. (47) for the complete sample of testing analytical solutions given in Eq. (46). One observes that the numerical solutions for the constant and linear fields (three first values in the respective equations) are as accurate as the Gauss-Legendre quadrature may lead to, according to the Theorem enounced before. The solutions for higher order potential fields show approximately the same accuracy whether using four or eight Gaussian points, as the threshold is actually the (lack of) ability of representing such fields with just 15 quadratic boundary elements.

A total of 81 points are distributed along the indicated dash line in Fig. 2 for the evaluation of results corresponding to the prescribed analytical solutions, as interpolated according to the assumed quadratic shape functions. Points 12 to 38 are actually outside the domain (inside the cavity) and should be accurately evaluated with zero values (see enlarged plot on the right of Fig. 2). Figure 3 shows the errors obtained for potential results evaluated along the indicated 81 points in Fig. 2 for the applied analytical solutions of Eq. (46) and using four Gaussian points. Target solutions are the analytical values as obtained for the open domain. One observes once more that the accuracy corresponds to the enounced Theorem and, most important, that such accuracy is not influenced by the proximity of a point to the boundary. Actually, as shown in the next example, the closer a point is to the boundary the more accurate the numerical results turn out to be, since the corresponding singularity is always evaluated within machine precision and independently from the Gauss-Legendre quadrature.

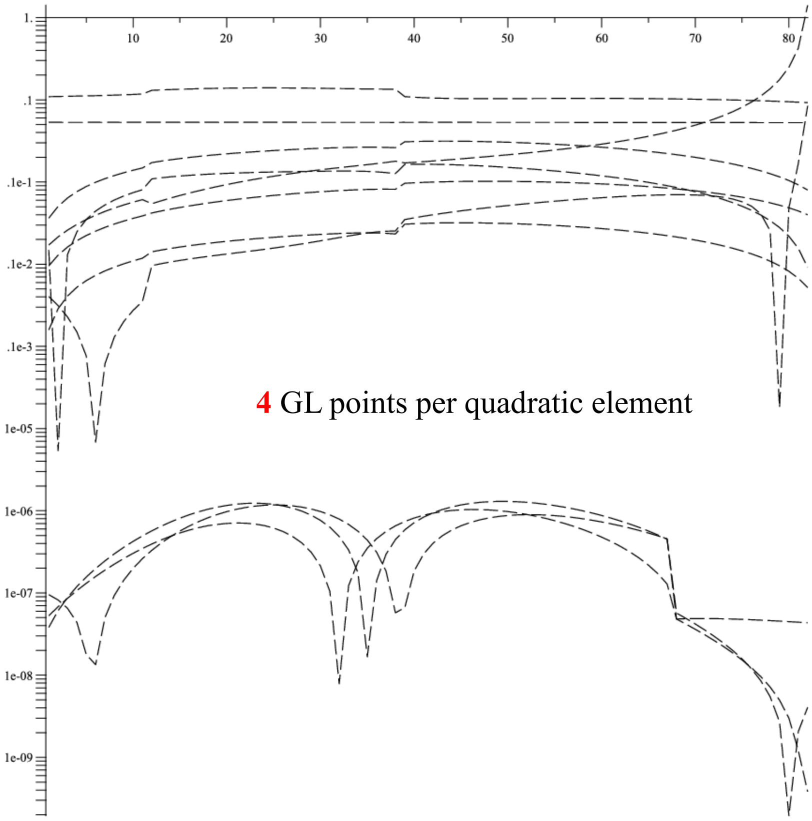

Figure 3. Error norms of internal potential results along the dash line in Fig. 2 obtained for potential and normal gradient values given for the 11 potential test fields of Eq. (46) and using four Gauss-Legendre points for integration along each element

7.2 Multiply-connected domain discretized with 10 cubic elements

Figure 4 shows a 2D domain discretized externally with six cubic elements and four more elements to configure a hole, in such a way that the Jacobian is always constant. Node four is almost coincident with the cavity boundary. The same 11 analytical fields of Eq. (46) are applied and in each case the corresponding nodal potential and gradient values $\mathbf{d}$ and $\mathbf{t}$, for the domain cut out as in Fig. 4, are evaluated in order to test the accuracy of Eq. (1). The corresponding error norms are the same ones of Eq. (47) and as previously described.

Proceedings of the XXXVIII Iberian Latin-American Congress on Computational Methods in Engineering
P.O. Faria, R.H. Lopez, L.F.F. Miguel, W.J.S. Gomes, M. Noronha (Editores), ABMEC, Florianópolis, SC, Brazil, November 5-8, 2017.

The matrices $\mathbf{G}$ and $\mathbf{H}$ were obtained using initially four Gaussian points per cubic element for all calculations. The orthogonality of $\mathbf{H}$ with respect to a constant potential field was checked with global Euclidean error ε_0, as in Eq. (47), of 10^{-11}, which is the first value shown in the following equation:

$$\langle 0.2e{-9} \quad 0.4e{-8} \quad 0.2e{-8} \quad 0.3e{-8} \quad 0.2e{-8} \quad 0.1e{-8} \quad 0.2e{-8} \quad 0.8e{-3} \quad 0.9e{-3} \quad 0.8 \quad 0.1\rangle \qquad (50)$$

In a second test with just one (!) Gaussian point, the corresponding Euclidean error ε_0 was 10^{-5}, as shown in the following:

$$\langle 0.2e{-3} \quad 0.2e{-2} \quad 0.3e{-2} \quad 0.2e{-2} \quad 0.2e{-2} \quad 0.3 \quad 0.6e{-1} \quad 0.1 \quad 1.2 \quad 3.4 \quad 1.1\rangle \qquad (51)$$

The remaining values in Eqs. (50) and (51) are Euclidean norms ε_1 defined in Eq. (47) for the complete sample of testing analytical solutions given in Eq. (46). One observes that, since one dealing with straight elements (better formulated: with constant Jacobians), the numerical solutions for up to cubic fields (seven first values in the respective equations) are as accurate as the Gauss-Legendre quadrature may lead to, according to the enounced Theorem when applied to constant Jacobians. The solutions for higher order potential fields obviously show significant differences in accuracy whether using four Gaussian points or just one.

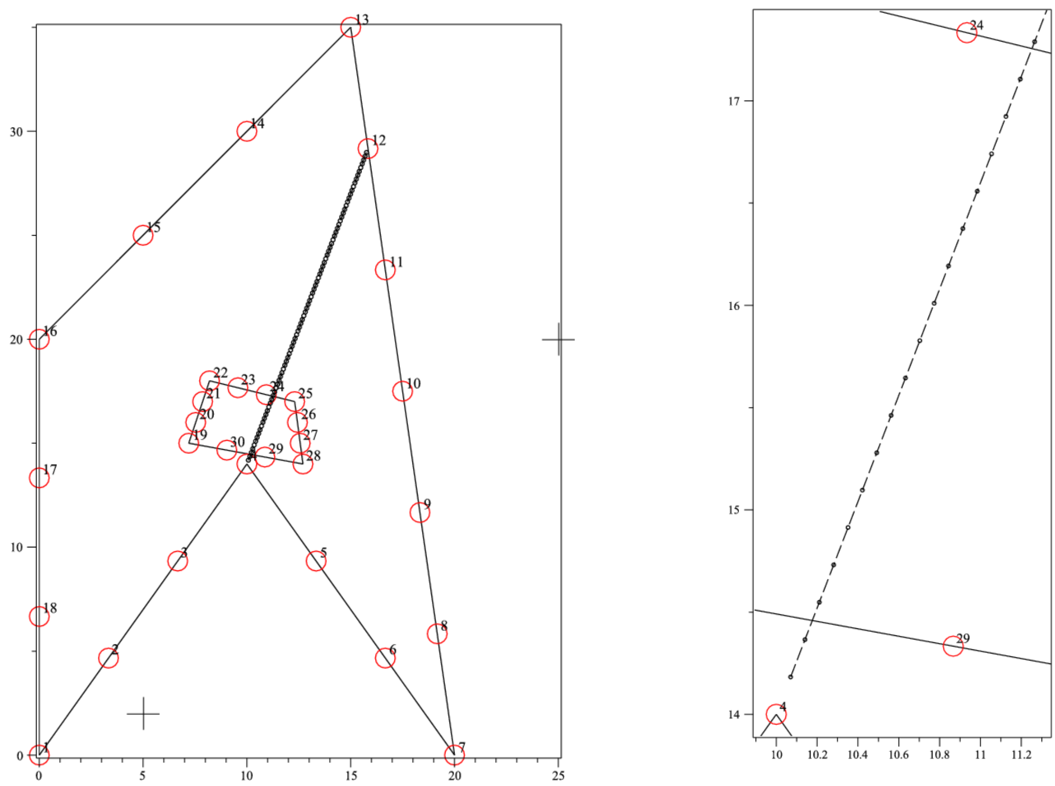

Figure 4. Multiply-connected domain discretized with a coarse mesh of 10 straight cubic elements and dash line along which internal results are evaluated (enlarged part displayed on the right)

A total of 81 points are distributed along the indicated dash line in Fig. 4 for the evaluation of results corresponding to the prescribed analytical solutions, as interpolated according to the assumed cubic shape functions. Points 3 to 17 are actually outside the domain, as they are placed inside the cavity, and should be accurately evaluated with zero values (see enlarged plot on the right of Fig. 4). Figure 5 shows the errors obtained for potential results evaluated along the indicated 81 points in Fig. 4 for the applied analytical solutions of Eq. (46) and using just one Gaussian point (since results with four Gaussian points just leads to too obvious results to be displayed). Target solutions are the analytical values as obtained for the open domain. One observes once more that the accuracy corresponds to the enounced Theorem and, what is really important, that the achieved accuracy for points close to the cavity – whether inside or outside – are evaluated to the ascribed computational precision of 20 digits. This in principle astounding results come from the fact that such points are considered in the code as complex quasi-singular when referred to all 10 cubic elements and, since the Jacobian is constant, the corresponding Gauss-Legendre quadrature can be carried out exactly with just one point. The points numbered higher than 40 are too far from the cavity elements to be considered quasi-singular and require only Gauss-Legendre quadratures.

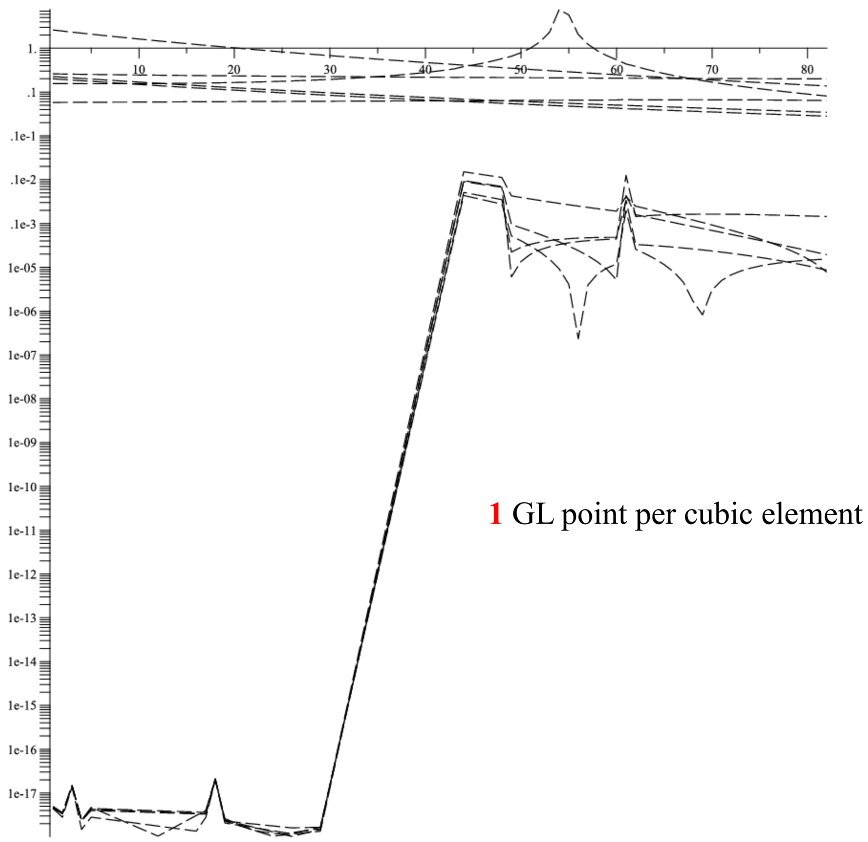

Figure 5. Error norms of internal potential results along the dash line in Fig. 4 obtained for potential and normal gradient values given for the 11 potential test fields of Eq. (46) and using only one Gauss-Legendre point for integration along each element

8 CONCLUDING REMARKS

This paper presents the collocation boundary element method exactly as it may be obtained from Somigliana's identity, but with a decisive improvement for generally curved boundaries, which leads to a theorem akin to the basic one of the displacement finite element method, namely that constant stress states must be represented exactly for an elastic isotropic medium. A practical outcome of the proposed improvement is that the logarithmic singularity of the single-layer potential matrix, for 2D problems, can always be dealt with analytically, with a remaining regular part that only requires a Gauss-Legendre quadrature. Such analytical results are actually independent from problem geometry and can be pre-evaluated and stored in tables for different element orders and numbers of quadrature points. General quasi-singularities – both for matrix assemblages and evaluation of results at internal points – are dealt with mathematically to an arbitrarily large accuracy, which completely dispenses with regularization techniques (including not always legitimate mechanical justifications) and artifacts such as interval subdivision and special quadrature schemes. It is in passing discussed that the qualifications *continuous* and *discontinuous*, as applied to boundary elements, are actually the result of misleading concepts and should not even be mentioned in relation to a consistent formulation, as presently proposed. Two simple – however convincing – numerical examples are displayed to just illustrate how remarkable the results can be in the present context, for instance with global or local errors never larger than 10^{-7} when using just four Gauss-Legendre quadrature points along curved quadratic elements independently from how high a singularity or quasi-singularity may occur. The example using cubic elements and straight boundary segments shows that actually just one integration point may be sufficient for a good accuracy of the results even (or, better said, particularly) when strong quasi-singularities are present.

ACKNOWLEDGEMENTS

This research work was supported by the Brazilian agencies CAPES, CNPq and FAPERJ.

REFERENCES

Bazeley, G. P., Cheung, Y. K., Irons, B. M. & Zienkiewicz, O. C., 1965. Triangular elements in bending – conforming and non-conforming solutions, In *Proc. Conf. Matrix Methods in Structural Mechanics*, Air Force Inst. Tech., Wright-Patterson A. F. Base, Ohio.

Brebbia, C. A., Telles, J. C. F. & Wrobel, L. C., 1984. *Boundary Element Techniques*, Springer-Verlag: Berlin and New York.

Dumont, N. A. & Noronha, M., 1998. A Simple, Accurate Scheme for the Numerical Evaluation of Integrals with Complex Singularity Poles. *Computational Mechanics*, vol. 22, n. 1, pp. 42-49.

Dumont, N. A., 1994. On the Efficient Numerical Evaluation of Integrals with Complex Singularity Poles. *Engineering Analysis with Boundary Elements*, vol. 13, pp.155-168.

Dumont, N. A., 1998. An assessment of the spectral properties of the matrix G used in the boundary element methods. *Computational Mechanics*, vol. 22, n. 1, pp. 32-41.

Dumont, N. A., 2010. The boundary element method revisited. In Brebbia, C. A., ed., *Boundary Elements and Other Mesh Reduction Methods XXXII*, pp. 227-238, WITPress, Southampton.

Dumont, N. A., 2017. The collocation boundary element method revisited: perfect code for 2D problems. *International Journal for Computational Methods and Experimental Measurements*, vol. 6, 11 pp.

Zienkiewicz, O. C., 1977. *The Finite Element Method*, McGraw-Hill.